Biodegradable Polyurethane Based on Random Copolymer of L-Lactide and ε-Caprolactone and Its Shape-Memory Property

Wenshou Wang,[1,2] Peng Ping,[1,2] Xuesi Chen,[1] Xiabin Jing[1]

[1]State key Laboratory of Polymer Physics and Chemistry, Changchun Institute of Applied Chemistry, Chinese Academy of Sciences, Changchun 130022, People's Republic of China
[2]Graduate School of Chinese Academy of Sciences, Beijing 100039, People's Republic of China

ABSTRACT: A series of biodegradable polyurethanes (PUs) are synthesized from the copolymer diols prepared from L-lactide and ε-caprolactone (CL), 2,4-toluene diisocyanate, and 1,4-butanediol. Their thermal and mechanical properties are characterized via FTIR, DSC, and tensile tests. Their T_gs are in the range of 28–53°C. They have high modulus, tensile strength, and elongation ratio at break. With increasing CL content, the PU changes from semicrystalline to completely amorphous. Thermal mechanical analysis is used to determine their shape-memory property. When they are deformed and fixed at proper temperatures, their shape-recovery is almost complete for a tensile elongation of 150% or a compression of 2-folds. By changing the content of CL and the hard-to-soft ratio, their T_gs and their shape-recovery temperature can be adjusted. Therefore, they may find wide applications. © 2007 Wiley Periodicals, Inc. J Appl Polym Sci 104: 4182–4187, 2007

Key words: shape memory; glass transition temperature; polyurethane; biodegradable

INTRODUCTION

As a new kind of smart material, shape-memory polymer has been studied and used in many fields because of its low cost and easy processing.[1–4] The shape-memory effect in polymers differs from those in ceramics and metals by the lower stress and larger recoverable strain achievable in polymers. Generally, a shape-memory polymer consists of two phases:[5,6] fixing phase determining the permanent shape and reversible phase fixing the temporary shape below the transition temperature. One of the first widely used shape-memory polymers is heat-shrink tubing.[7] As the development of research, corresponding characterization and constitutive modeling of the thermomechanical shape-memory cycle are developed,[8–11] and medical devices and microsystem components based on the shape-memory polymer are created.[12–16] Since Lendlein and Langer prepared shape-memory polyurethane (PU)[17] based on poly(ε-caprolactone) (PCL) and predicted its potential usage in medical treatment, shape-memory polymers with excellent biodegradation and biocompatibility properties have attracted much research attention. Most of biodegradable shape-memory polymers reported recently are based on PCL, co-oligoesters of (rac-) lactide and glycolide, or others.[17–20] They all show good shape-memory properties, but their shortcomings are obvious. Either they have low recovery stress or they have poor mechanical strength after shape recovery. Polylactide, as well known, has been widely studied because of its biodegradability and excellent mechanical property. But its glass transition temperature (T_g) is about 60°C, and cannot get a complete recovery near the body temperature. So we try to use the co-oligomer of lactide (LA) and ε-caprolactone (CL) as soft segments. On one hand, the incorporation of CL may decrease the T_g of the soft segment and improve the mechanical properties; on the other hand, we can adjust the degradation speed through controlling the weight fraction of CL.[21,22]

In this study, using the co-oligomer of LA and CL (PCLA) as soft segment, 2,4-toluene diisocyanate (TDI) as hard segment, and 1,4-butanediol (BDO) as chain extender, a series of such biodegradable PUs were prepared. Molecular weight (M_n) of the PCLA was 5000, the weight fraction of CL in PCLA was from 20 to 5%, and the molar ratio of PCLA/TDI/BDO was from 1/3/2 to 1/7/6. The thermal and mechanical properties and shape memory effect of the PUs were studied.
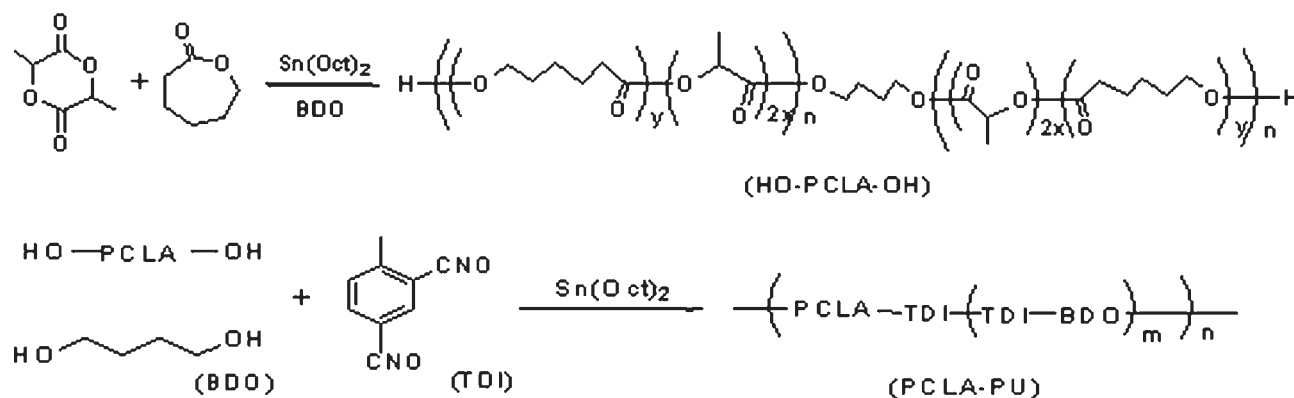
Scheme 1 Synthesis route of PCLA-PU.

EXPERIMENT

Materials

L-lactide was purchased from Purac, Holland. BDO and stannous octoate (Sn(Oct)$_2$, 95%) were purchased from Aldrich. Toluene was dried over Na wire and distilled before use. Ethyl acetate and TDI were purchased from North-China Chemical and were distilled prior to use. CL was distilled over freshly powdered calcium hydride under reduced pressure.

Preparation of PCLA diol and PUs

After three times of recrystallization from ethyl acetate, L-lactide was added into a glass ampoule, which had been flame-dried and equipped with a magnetic stirring bar, and then BDO and CL were added. Finally an equal amount of toluene and Sn(Oct)$_2$ (0.3% of the BDO, mol/mol) in toluene solution were injected into the ampoule through a syringe. The reaction vessel was immersed into a thermostatic oil bath at 125°C for 24 h. Then, the product (PCLA diol) was precipitated into ethanol and dried under vacuum for 48 h.

The general synthesis procedure of PUs is as follows (see Scheme 1): a certain amount of PCLA diol was dissolved in double volumes of toluene and heated at 65°C for 20 min. Sn(Oct)$_2$ (0.8% of the PCLA diol, mol/mol) in dried toluene and a given amount of TDI were added to the solution. After 10 min at 65°C, BDO, the mole number of which was equal to the molar difference between TDI and PCLA diol, was added and the reaction mixture was stirred for another 6 h. The polymer was isolated by dissolving the reaction mixture in chloroform, followed by precipitation in ethanol.

Measurements

The molecular weights and molecular weight distribution of the polymers prepared were analyzed by gel permeation chromatography (GPC, Waters 410) in chloroform solution at 25°C. The molecular weights were calibrated against polystyrene standards. Infrared spectra of the PU films were taken on a Bruker Vertex 70 FTIR with a resolution of 4 cm^{-1} and a scan number of 32. ^{1}H NMR spectra were recorded on a Bruker AV 400 MHz at room temperature with CDCl$_3$ as solvent. Differential scanning calorimetry (DSC) was carried out over a temperature range of 10–200°C using a Perkin-Elmer DSC-7 purged with nitrogen. The heating or cooling rate was 10°C/min. Tensile tests were conducted on an Instron 1121 at a rate of 20 mm/min at room temperature. Five dumbbell-shaped specimens (effective dimension 4 × 0.7 mm^2) of the same kind were tested to get mean values.

The shape-memory property of the PUs was examined for both tensile and compression deformations. Dumbbell-shaped specimens (effective dimension 4 × 0.7 mm^2) were used for tensile tests. They were mold-pressed at 140–180°C. The tensile deformation was realized on Instron 1121 equipped with a temperature-controlled thermal cabinet. The specimen was elongated 150% at the temperature about 5° above its T_g and then cooled quickly at the temperature 15° below its T_g. For a simple recovery-ratio measurement, the stretched specimen was put in a water bath. When the water was heated to a certain temperature,

TABLE I
GPC Results of PCLAs and PUs

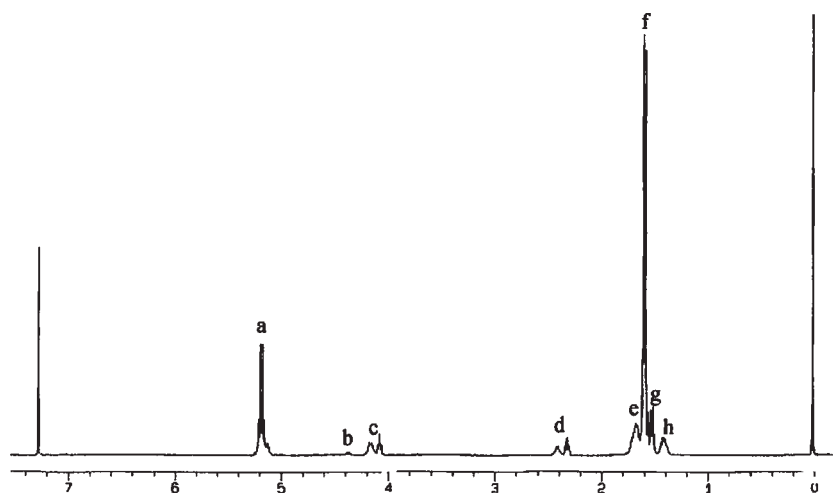| Polymer code	M_w (10^3)	M_n (10^3)	M_w/M_n
PCLA20	5.24	4.76	1.10
PCLA20-PU132	99.4	56.7	1.75
PCLA20-PU154	182.4	87.9	2.07
PCLA20-PU176	165.8	88.6	1.87
PCLA10	5.33	4.98	1.07
PCLA10-PU132	283.1	164.8	1.72
PCLA10-PU154	271.3	155.0	1.75
PCLA10-PU176	314.4	186.8	1.68
PCLA5	5.57	5.16	1.08
PCLA5-PU132	95.8	53.8	1.78
PCLA5-PU154	132.9	69.3	1.92
PCLA5-PU176	107.5	69.2	1.55

Figure 1 ^{1}H NMR spectrum of PCLA20.

the specimen began to shrink and get a little bent, and then became straightened gradually again. When the specimen looked completely straightened, the bath temperature was taken as the recovery temperature RT and specimen length was measured to calculate the recovery ratio. For the measurement of restoration force, the stretched specimen was cooled to room temperature under extension and released from the clamps. Then the specimen was clamped in the tester again. With its length fixed, the specimen was heated at 3°C/min until 60°C and the tensile stress was recorded as restoration force.

For compressed specimens, the shape-memory property was examined by thermal mechanical analysis (TMA). A cylinder of φ 2 mm cut from a 2 mm thick PU plate was compressed into a 1 mm thick disk at the temperature about 5°C above T_g and then cooled quickly to the temperature 20°C below the processing temperature. The TMA was conducted on a Perkin–Elmer DMA-7 in the temperature range of

10–70°C at a heating rate of 3°C/min. The disk thickness was recorded as a function of temperature.

RESULTS AND DISCUSSION

Synthesis of PCLA diols and PCLA-PUs

Three PCLA diols and nine PCLA-PUs were synthesized by the aforementioned method. After desiccation, they were characterized by GPC, ^{1}H NMR, and FTIR. The precipitated PCLA-PUs are white flocs. They can dissolve in chloroform well. Their molecular weights are shown in Table I. The molecular weights of the three PCLA diols are approximately 5000. The CL contents are 20, 10, and 5 mol %, respectively, according to the feed composition. They are coded as PCLA20, PCLA10, and PCLA5, respectively, in Table I. For each PCLA diol, three molar ratios of PCLA/TDI/BDO were used, i.e., 1/3/2, 1/5/4, and 1/7/6. Therefore, the PUs are coded as PU132, PU154, and PU176, respectively.
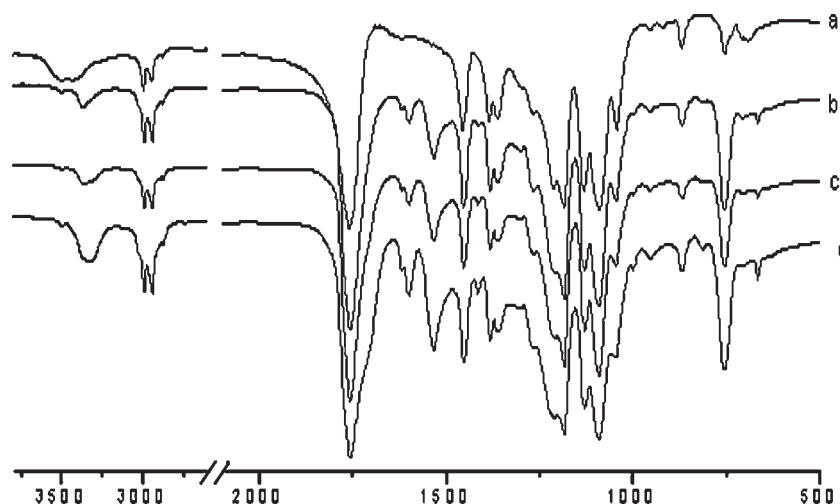

Figure 2 FTIR spectra of (a) PCLA20, (b) PCLA20-PU132, (c) PCLA20-PU154, and (d) PCLA20-PU176.

TABLE II
DSC Results of the PCLAs and PUs

Samples	T_g (°C)	T_c (°C)	T_m (°C)	ΔH_c (J/g)	ΔH_m (J/g)	X_c (PLA)[a] (%)
PCLA20	19					
PCLA20-PU132	28					
PCLA20-PU154	36					
PCLA20-PU176	40.2					
PCLA10	37.7	105	132	−5.2	6.4	6.7
PCLA10-PU132	43		130		2.3	2.9
PCLA10-PU154	48		131		0.6	0.83
PCLA10-PU176	53		131		0.2	0.30
PCLA5	42	106.9	133	−11.9	20.8	21.9
PCLA5-PU132	52.6	107.4	132.8	−1.3	3.3	4.0
PCLA5-PU154	46.8	103.2	132	−3.5	7.9	10.4
PCLA5-PU176	50		133		3.3	4.7

[a] X_c(PLA) is calculated according to the following equation.[24] $X_c = \Delta H_m/100$ where ΔH_m is the measured fusion enthalpy of the sample, and 100 (J/g) is the theoretical fusion enthalpy of PLA crystals.[25]

NMR

Figure 1 shows the ^{1}H NMR of PCLA20. Peaks a and f are corresponding to chemical shifts of CH and CH_3 of the LA unit, and peaks d, e, h, g, and c are corresponding to the chemical shifts of the CL unit. The detailed codes are shown in Figure 1. From the ^{1}H NMR results, it is concluded that the CL and LA are copolymerized randomly. So the addition of CL can decrease the T_g of PLA effectively, as can be proved by the following DSC results.

FTIR spectroscopy

Typical FTIR spectra of PCLA diol and PUs are shown in Figure 2. PCLA diol has two typical peaks at 3523 cm^{-1} (OH stretching) and 1763 cm^{-1} (C=O stretching). In the PUs, the peak at 3523 cm^{-1} disappears while two new peaks appear at 3353 cm^{-1} (NH stretching) and 1534 cm^{-1} (Amide II). The absorbance intensities of these new peaks increase with increasing hard segment content. All these spectral changes provide convincing evidence for the formation of PU.

DSC analyses

Thermal behaviors of the PCLAs and PUs were investigated by DSC. The CL content has a great influence on PCLAs. When the weight fraction of CL increases from 5 to 20%, the semicrystalline PCLA becomes amorphous completely and its T_g decreases from 42 to 19°C. This is understandable, because the addition of flexible CL destroys regularity of the PLA chains, makes their crystallization difficult and results in more free volume for glass transition. As shown in Table II, the T_gs of all PUs are higher than those of corresponding PCLA diols due to the restraints from the hard segments in PUs. For a given PCLA soft segment, the T_g of PU increases with increasing content of the hard segment. The only exception is sample PCLA5-PU154. It has the lowest T_g among the three of the PCLA5 group. This can be explained as follows. As to the T_gs of the PUs, two effects should be considered: one is the constraint received by the PCLA segments from the hard segments, which leads to higher T_g of the PCLA domains; the other is the phase separation, the degree of which determines the interaction between the soft and hard segments and may cause decrease in T_g of PCLA phase. PCLA5-PU154 has a relatively high crystallinity (Table II). It implies more phase separation in it. The observed lower T_g indicates that the phase separation effect overwhelms the interphase restraint.

Mechanical properties

Tensile properties of the various PUs prepared are shown in Figure 3 and Table III. Table III shows that for a given PU composition such as PU176, the tensile strength and modulus increase and elongation at break decreases when the CL content in the soft seg-
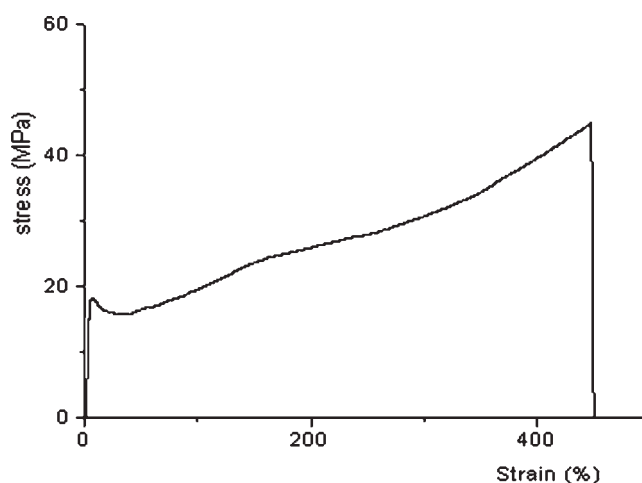

Figure 3 Typical stress–strain curve of PCLA20-PU176.

TABLE III
Tensile Test Results of the PUs

Samples	Strength (MPa)	Modulus (MPa)	Elongation at break (%)
PCLA5-PU176	50	1163	99
PCLA10-PU176	48	1000	245
PCLA20-PU176	43	740	440
PCLA20-PU154	36	580	456
PCLA20-PU132	25	360	385

ment increases from 5 to 20%. Among the group of PCLA20, the tensile strength, modulus, and elongation at break all increase with increasing hard segment length. In other words, both CL content in the soft segments and the hard-to-soft ratio can govern the physical properties of the final products. This is due to the fact that there are rich hydrogen bonds and dipole–dipole interactions in the hard domains and they can strengthen the materials. And incorporation of flexible CL units reduces the molecular chain regularity and enhances their mobility. Compared with the PCLUs,[18] their elongations at break decreases a little, but their tensile strength and modulus improve greatly.

Shape memory behavior

Shape memory PUs often have a two-phase structure, namely, the fixing phase (having a high phase transition temperature T_{high}) remembers the initial shape and the reversible phase (having a low phase transition temperature T_g or T_m) shows a reversible rigid-to-soft transition. The melting peak of PCL is not observed in all PCLAs and PUs, showing that CL is incorporated in PLA and not homopolymerized. So the shape memory effects of the PUs are based on their T_gs not on their T_ms. Similar to other shape-memory polymers based on T_g,[23] it is deformed at a temperature (DT) above its T_g and the deformation is fixed at a temperature (FT) below its T_g. In the present study, tensile test and TMA are employed to examine the shape-memory effects. The procedure for tensile test is "150% elongation at DT—fixation at FT—recov-
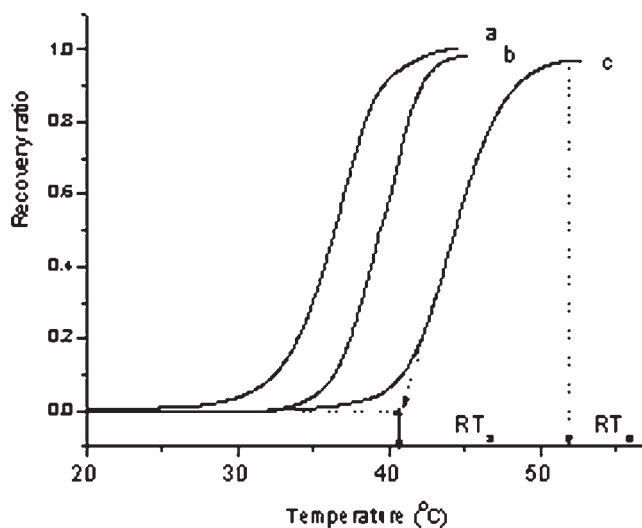

Figure 4 Typical TMA curves of (a) PCLA10-PU132, (b) PCLA10-PU154, and (c) PCLA10-PU176.

ery at RT." Typical DT, FT, RT, and recovery ratio data are collected in Table IV for various PU samples. In TMA, sample thickness is measured as a function of temperature for a compressed specimen. Therefore, it can reveal the shape-recovery process and give the start temperature (RT_s) and end temperature (RT_e) shown in Figure 4. Under the condition of "2 folds compression at DT—fixation at FT," the measured RT_s and RT_e and the recovery ratio are listed in Table V.

Tables IV and V show that the PU samples have good shape recovery ratios (above 93%) no matter they are evaluated in tensile mode or compression mode. Generally speaking, under the condition of "deformation at $T_g + 5°C$ and fixation at $T_g - 15°C$," the RTs determined are $T_g \pm 1.5°C$ for tensile tests (Table IV) and $T_g \pm 2.0°C$ for TMA (Table V, RT_e). In short, T_gs determine their recovery temperatures. By changing the CL content in the PCLA diols and changing the hard-to-soft segment ratio, it is possible to adjust the T_g and the recovery temperature over a range of 30–55°C. As shown in Tables IV and V, sample PCLA20-PU154 and PCLA20-PU176 show their RT near the body temperature. They display

TABLE IV
Shape-Memory Data of PUs Evaluated by Tensile Test

Samples	T_g (°C)	DT (°C)	FT (°C)	RT (°C)	Recovery ratio (%)	T_{max} (°C)	F_{max} (MPa)
PCLA20-PU132	28	33	13	30	100	22	1.38
PCLA20-PU154	36	41	21	35	97	32	2.66
PCLA20-PU176	40.2	45	25	39	94	36	3.52
PCLA10-PU132	43	48	28	42	100	35	2.07
PCLA10-PU154	48	53	33	44	96	42	3.86
PCLA10-PU176	53	58	38	52	93	49	4.60
PCLA5-PU132	52.6	58	38	53	100	47	3.12
PCLA5-PU154	46.8	52	32	49	95	43	4.26
PCLA5-PU176	50	55	35	51	93	48	5.50

TABLE V
Shape-Memory Data of PUs Evaluated by TMA

Samples	T_g (°C)	DT (°C)	FT (°C)	RT_s (°C)	RT_e (°C)	Recovery ratio (%)
PCLA20-PU132	28	33	13	17	31	100
PCLA20-PU154	36	41	21	26	37	98
PCLA20-PU176	40.2	45	25	28	39	96
PCLA10-PU132	43	48	28	33	44	100
PCLA10-PU154	48	53	33	36	45	97
PCLA10-PU176	53	58	38	41	52	97
PCLA5-PU132	52.6	58	38	41	55	100
PCLA5-PU154	46.8	52	32	36	50	96
PCLA5-PU176	50	55	35	40	52	95

satisfactory tensile strength and elongation at break (Table III). Therefore, they are expected to have a potential application in medical treatments.

Restoration force is an important factor to a shape memory material. So we tested the maximum restoration forces (F_{max}) and the temperatures (T_{max}) having the F_{max} of all PUs prepared (Fig. 5, Table IV). It is seen that the F_{max} is dependent on both CL content in PCLA and PU composition. For a given PU composition, the F_{max} decreases with increasing CL content in PCLA diols. For a given PCLA, the F_{max} increases with increasing hard segment length. As a whole, all PCLA-based PUs show much higher F_{max}s than those of corresponding PCL-based PUs.[18]

CONCLUSIONS

We have synthesized a series of biodegradable PUs based on PCLA diols, TDI, and BDO. They display excellent mechanical properties. Their T_gs are in the range of 28–53°C, influenced by the CL content in PCLA and the ratio of soft segment to hard segment. When they are deformed at $T_g + 5$°C and fixed at $T_g -$

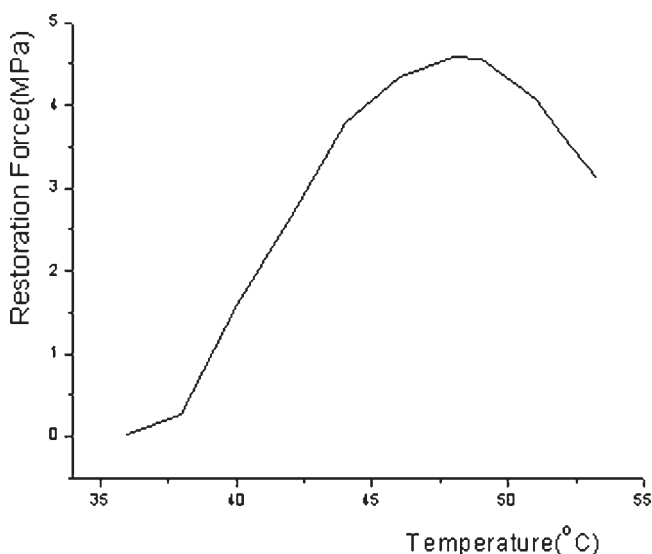15°C, their shape-recovery ratios are more than 93% for a tensile elongation of 150% or a compression of 2-folds. Their complete shape-recovery temperatures are $T_g \pm 1.5$°C for tensile tests and $T_g \pm 2.0$°C for TMA. They show considerable restoration forces, their T_gs and shape-recovery temperatures can be lowered to the body temperature easily. Therefore, they are expected to find practical medical applications.

Figure 5 Typical restoration force–temperature curves of PCLA10PU176.

References

1. Liu, C. D.; Chun, S. B.; Mather, P. T.; Zheng, L.; Haley, R. H.; Coughlin, R. B. Macromolecules 2002, 35, 9868.
2. Liu, Y.; Gall, K.; Dunn, M. L.; McCluskey, P. Smart Mater Struct 2003, 12, 947.
3. El Feninat, F.; Laroche, G.; Fiset, M.; Mantovani, D. Adv Eng Mater 2002, 4, 91.
4. Lin, J. R.; Chen, L. W. J Appl Polym Sci 1998, 69, 1575.
5. Liang, C.; Rogers, C. A.; Malafeew, E. J Intell Mater Struct 1997, 8, 380.
6. Richard, F.; Gordon, P. E. Mater Technol 1993, 8, 254.
7. Ota, S. Rad Phys Chem 1981, 18, 81.
8. Bhattacharyya, A.; Tobushi, H. Polym Eng Sci 2000, 40, 2498.
9. Lin, J. R.; Chen, L. W. J Appl Polym Sci 1999, 73, 1305.
10. Bonart, R. Polymer 1979, 20, 1389.
11. Lendlein, A.; Kelch, S. Angew Chem Int Ed 2034 2002, 41.
12. Metzger, M. F.; Wilson, T. S.; Schumann, D.; Mathews, D. L. Biomed Microdevices 2002, 4, 89.
13. Maitland, D. J; Metzger, M. F.; Schumann, D.; Lee, A.; Wilson, T. S. Lasers Sur Med 2002, 30, 1.
14. Gall, K.; Yakachi, C. M.; Liu Y. P.; Shandas, R.; Willett, N.; Anseth, K. S. J Biomed Mater Res Part A 2005, 73A, 339.
15. Gall, K.; Kreiner, P.; Turner, D.; Hulse, M. J MEMS 2004, 13, 472.
16. Ferrera, D.A. US Pat No 6,224,610, 2001.
17. Lendlein, A.; Langer, R. Science 2002, 296, 1673.
18. Ping, P.; Wang, W. S.; Chen, X. S.; Jing, X. B. Biomacromolecules 2005, 6, 587.
19. Armin, A.; Yakai, F.; Steffen, K.; Andreas, L. Angrew Chem Int Ed 2005, 44, 1188.
20. Kim, Y. B.; Chung, C. W.; Kim, H. W.; Rhee, Y. H. Macromol Rapid Commun 2005, 26, 1070.
21. Ye, W. P.; Du, F. S. Jin, J. Y. Reac Func Polym 1997, 32, 161.
22. Malin, M.; HiljanenVainio, M.; Karjalainen, T. J Appl Polym Sci 1996, 59, 1289.
23. Byung, K. K.; Young, J. S.; Seong, M. C.; Han, M. J. J Polym Sci Polym Phys 2000, 38, 2652.
24. Tsuji, H.; Ishida, T. J Appl Polym Sci 2003, 87, 1628.
25. Huang, J.; Lisowski, M. S.; Runt, J.; Hall, E. S.; Kean, R. T.; Buehler, N.; Lin, J. S. Macromolecules 1998, 31, 2593.